

Designing 3-D Molecular Stars

William Tiznado,[†] Nancy Perez-Peralta,[‡] Rafael Islas,[‡] Alejandro Toro-Labbe,[§]
Jesus M. Ugalde,[‡] and Gabriel Merino^{*‡}

Departamento de Ciencias Químicas, Facultad de Ecología y Recursos Naturales, Universidad Andres Bello, Av. República 275, Santiago-Chile, Departamento de Química, División de Ciencias Naturales y Exactas, Universidad de Guanajuato, Col. Noria Alta s/n C.P. 36050, Guanajuato, Gto., México, QTC, Departamento de Química Física, Facultad de Química, Pontificia Universidad Católica de Chile, Casilla 306, Correo 22, Santiago, Chile, and Kimika Fakultatea, Euskal Herriko Unibertsitatea and Donostia International Physics Center (DIPC), P.K. 1072, 20080 Donostia, Euskadi, Spain

Received May 17, 2009; E-mail: gmerino@quijote.ugto.mx

Abstract: We have explored in detail the potential energy surfaces of the $\text{Si}_5\text{Li}_n^{5-6}$ ($n = 5-7$) systems. We found that it is feasible to design three-dimensional star-like silicon structures using the appropriate ligands. The global minimum structure for Si_5Li_7^+ has a perfect seven-peak star-like structure. The title compounds comprise, essentially, the Si_5^{6-} ring interacting with lithium cations. The ionic character of the Si–Li interactions induces the formation of a bridged structure. Concomitantly, our calculations show that the reduction of the Pauli repulsion and the maximization of the orbital contribution are also significant for the star-like structure formation. Additionally, the MO analysis of the systems suggests that the role of the lithium atoms is to provide the precise number of electrons to the central Si_5 unit. This is confirmed by the magnetic properties, which show that electron delocalization enhances the stability of the star-like structures proposed here.

Introduction

Molecules made by main group elements comprise a number of interesting examples of unstable, strained, distorted, sterically hindered, bent, and battered structures.¹ Chemists have always been fascinated by these atypical molecular structures, not only for the challenge of devising and synthesizing them but also because they often stem from a type of unusual chemical bonding. For instance, in 1970 Hoffmann, Alder, and Wilcox suggested some rules to stabilize molecules containing a tetracoordinate carbon in an unorthodox situation: just planar (i.e., planar tetracoordinate carbon molecules).² Inspired by Hoffmann's ideas, several groups have successfully suggested and experimentally characterized molecules containing a planar hypercoordinate center.^{3–8}

The groups of Schleyer⁹ and Minkin¹⁰ proposed a series of beautiful perlithioannulenes C_nLi_n ($n = 3-6$) with planar star-

like structures. However, some of them are just local minima on the corresponding potential energy surfaces.^{11–13} Similar bridged structures have been proposed for Si_6Li_6 ¹⁴ and $\text{B}_6\text{H}_6\text{Li}_6$,^{15,16} but in the particular case of Si_6Li_6 , the D_{6h} structure is only a local minimum.^{17,18} In contrast, lithiation converts the octahedron $\text{B}_6\text{H}_6^{2-}$ cluster in a planar aromatic benzene-like structure.^{15,16}

One lesson that organic chemistry teaches us is that high-energy isomers (cubane, for example) are just as interesting as global minima (e.g., styrene in the C_8H_8 family).¹⁹ However, in the case of clusters, gas-phase methods under “annealing” conditions tend to generate only lowest-energy isomers. Recently, in a couple of reports,^{20,21} the groups of Wang and Boldyrev discussed in detail the importance of looking for global minimum structures rather than seeking nice hypercoordinate

[†] Universidad Andres Bello.
[‡] Universidad de Guanajuato.
[§] Pontificia Universidad Católica de Chile.
[‡] Euskal Herriko Unibertsitatea and Donostia International Physics Center (DIPC).
(1) Hoffmann, R.; Hopf, H. *Angew. Chem., Int. Ed.* **2008**, *47*, 4474.
(2) Hoffmann, R.; Alder, R.; Wilcox, C. F., Jr. *J. Am. Chem. Soc.* **1970**, *92*, 4992.
(3) Keese, R. *Chem. Rev.* **2006**, *106*, 4787.
(4) Merino, G.; Mendez-Rojas, M. A.; Vela, A.; Heine, T. *J. Comput. Chem.* **2007**, *28*, 362.
(5) Collins, J. B.; Dill, J. D.; Jemmis, E. D.; Apeloig, Y.; Schleyer, P. v. R.; Seeger, R.; Pople, J. A. *J. Am. Chem. Soc.* **1976**, *98*, 5419.
(6) Radom, L.; Rasmussen, D. R. *Pure Appl. Chem.* **1998**, *70*, 1977.
(7) Siebert, W.; Gunale, A. *Chem. Soc. Rev.* **1999**, *28*, 367.
(8) Sorger, K.; Schleyer, P. v. R. *J. Mol. Struct. (THEOCHEM)* **1995**, *338*, 317.

(9) Jemmis, E. D.; Subramanian, G.; Kos, A. J.; Schleyer, P. v. R. *J. Am. Chem. Soc.* **1997**, *119*, 9504.
(10) Minkin, V. I.; Minyaev, R. M.; Starikov, A. G.; Gribanova, T. N. *Russ. J. Org. Chem.* **2005**, *41*, 1289.
(11) Bachrach, S. M.; Miller, J. V. *J. Org. Chem.* **2002**, *67*, 7389.
(12) Smith, B. J. *Chem. Phys. Lett.* **1993**, *207*, 403.
(13) Xie, Y. M.; Schaefer, H. F. *Chem. Phys. Lett.* **1991**, *179*, 563.
(14) Santos, J. C.; Fuentealba, P. *Chem. Phys. Lett.* **2007**, *443*, 439.
(15) Alexandrova, A. N.; Birch, K. A.; Boldyrev, A. I. *J. Am. Chem. Soc.* **2003**, *125*, 10786.
(16) Alexandrova, A. N.; Boldyrev, A. I. *Inorg. Chem.* **2004**, *43*, 3588.
(17) Zdetsis, A. D. *J. Chem. Phys.* **2007**, *127*, 214306.
(18) Zdetsis, A. D.; Fowler, P. W.; Havenith, R. W. A. *Mol. Phys.* **2008**, *106*, 1803.
(19) Eaton, P. E.; Cole, T. W. *J. Am. Chem. Soc.* **1964**, *86*, 3157.
(20) Averkiev, B. B.; Zubarev, D. Y.; Wang, L. M.; Huang, W.; Wang, L. S.; Boldyrev, A. I. *J. Am. Chem. Soc.* **2008**, *130*, 9248.
(21) Wang, L. M.; Huang, W.; Averkiev, B. B.; Boldyrev, A. I.; Wang, L. S. *Angew. Chem., Int. Ed.* **2007**, *46*, 4550.

structures,^{22,23} since only global minimum structures or low-lying isomers can be experimentally observed under annealing conditions. Thus, the quest of the lowest-energy structures becomes relevant to address future experimental confirmation.

Binary clusters containing silicon atoms have been studied extensively. Particularly, mixed transition metal silicon clusters have been the object of experimental studies by mass spectrometry²⁴ or by photoelectron spectroscopy.²⁵ The study of alkali–silicon clusters is also of significant interest. Alkali metals adsorbed on semiconductor surfaces are attractive because they work as a promoter in catalysts.^{26–28} Obviously, the study of alkali–silicon clusters could furnish a better understanding in the interaction between silicon and alkali atoms and could help to find the best sites of adsorption. However, only small lithium- and sodium-doped silicon clusters have been investigated.^{29–34} For instance, the ionization potentials of Si_nNa_m , ($3 \leq n \leq 11$; $1 \leq m \leq 4$), have been experimentally determined from the threshold energies of their ionization efficiency curves.^{33,34}

Herein, we analyze the stability, the electronic structure, and the bonding patterns of a selected group of silicon–lithium clusters. We have found that it is feasible to design a three-dimensional star-like silicon structure using the appropriate ligands. In particular, we found that the most stable structure for Si_3Li_7^+ has a perfect seven-peak star-like structure.

Computational Details

Potential energy surfaces were scanned with the use of the gradient embedded genetic algorithm (GEGA) program.^{35,36} We used the B3LYP^{37,38} functional as is implemented in the Gaussian 03 program³⁹ with the SDD⁴⁰ basis sets for energy, gradient, and force calculations. We reoptimized geometries and calculated frequencies for all isomers found for the title complexes at the B3LYP/def2-TZVPP⁴¹ level. Total energies of the local minimum structures were also recalculated at the CCSD(T)⁴²/def2-TZVPP//B3LYP/def2-TZVPP level. To analyze the bonding mechanism, a

natural population analysis (NPA)⁴³ was done. Wiberg bond indices (WBI) were also computed.

To gain more insight into the nature of the bonding in these star-like systems, an energy decomposition analysis,^{44–46} EDA, was performed as implemented in the ADF2008.01 package.^{47,48} The overall bond energy, ΔE , corresponding to the formation of a molecule from two (or sometimes more) fragments is divided into two major components (see eq 1).

$$\Delta E = \Delta E_{\text{prep}} + \Delta E_{\text{int}} \quad (1)$$

The preparation energy, ΔE_{prep} , corresponds to the energy required to deform the separated fragments from their equilibrium structures to the geometries they acquire into the molecule. The interaction energy, ΔE_{int} , corresponds to the actual energy generated when the deformed fragments are combined into the overall molecule. It is further divided into three physical meaningful terms (see eq 2): the Pauli repulsion, ΔE_{Pauli} ; the classical electrostatic interaction, ΔV_{elstat} ; and the orbital interaction energy, ΔE_{oi} .

$$\Delta E_{\text{int}} = \Delta E_{\text{Pauli}} + \Delta V_{\text{elstat}} + \Delta E_{\text{oi}} \quad (2)$$

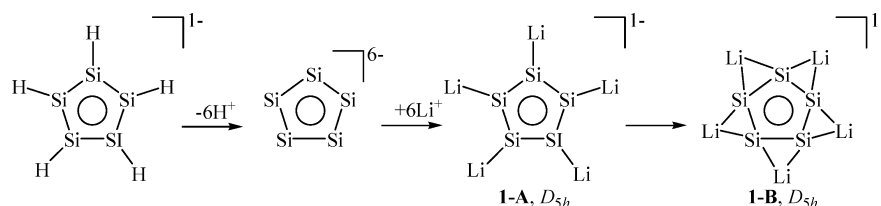
In the present work, the nature of the bonding in structures **3A** and **3B** was analyzed using EDA; both systems were separated into two fragments, $\text{Si}_5\text{Li}_2^{4-}$ and Li_5^{5+} , whose structures were taken from the Gaussian 03 geometry optimizations. The EDA calculations were carried out using the exchange functional of Becke³⁷ with the correlation functional of Perdew⁴⁹ in ADF2008.01. The basis sets have triple- ζ quality augmented by two sets of polarization functions, that is, d and f functions for lithium and silicon atoms. Scalar relativistic effects were considered using the zero-order regular approximation (ZORA).

The induced magnetic field (\mathbf{B}^{ind}) calculations were performed using PW91 functional in conjunction with the IGLO-III basis set for silicon and IGLO-II for lithium.⁵⁰ We refer to this basis set by the acronym IGLO. The shielding tensors were computed using the IGLO method.⁵¹ The deMon program was used to compute the molecular orbitals,⁵² and the deMon-NMR package, for the shielding tensors.⁵³ Induced magnetic fields were computed in ppm of the external field applied perpendicular to the molecular plane. Assuming an external magnetic field of $|\mathbf{B}^{\text{ext}}| = 1.0$ T, the unit of \mathbf{B}^{ind} is $1.0 \mu\text{T}$, which is equivalent to 1.0 ppm of the shielding tensor. In order to render the induced magnetic fields the molecules were oriented so that the center of mass located at the origin of the coordinate system; the z-axis is parallel to the highest-order symmetry axis of the molecule. The external field is applied

- (22) Exner, K.; Schleyer, P. v. R. *Science* **2000**, *290*, 1937.
 (23) Islas, R.; Heine, T.; Ito, K.; Schleyer, P. v. R.; Merino, G. *J. Am. Chem. Soc.* **2007**, *129*, 14767.
 (24) Beck, S. M. *J. Chem. Phys.* **1989**, *90*, 6306.
 (25) Ohara, M.; Koyasu, K.; Nakajima, A.; Kaya, K. *Chem. Phys. Lett.* **2003**, *371*, 490.
 (26) Fong, C. Y.; Yang, L. H.; Batra, I. P. *Phys. Rev. B* **1989**, *40*, 6120.
 (27) Glander, G. S.; Webb, M. B. *Surf. Sci.* **1989**, *222*, 64.
 (28) Souda, R.; Hayami, W.; Aizawa, T.; Otani, S.; Ishizawa, Y. *Phys. Rev. Lett.* **1992**, *69*, 192.
 (29) Sporea, C.; Rabilloud, F.; Allouche, A. R.; Frecon, M. *J. Phys. Chem. A* **2006**, *110*, 1046.
 (30) Sporea, C.; Rabilloud, F.; Cosson, X.; Allouche, A. R.; Aubert-Frecon, M. *J. Phys. Chem. A* **2006**, *110*, 6032.
 (31) Sporea, C.; Rabilloud, F. *J. Chem. Phys.* **2007**, *127*, 164306.
 (32) Sporea, C.; Rabilloud, F.; Aubert-Frecon, M. *J. Mol. Struct. (THEOCHEM)* **2007**, *802*, 85.
 (33) Kishi, R.; Iwata, S.; Nakajima, A.; Kaya, K. *J. Chem. Phys.* **1997**, *107*, 3056.
 (34) Kishi, R.; Kawamata, H.; Negishi, Y.; Iwata, S.; Nakajima, A.; Kaya, K. *J. Chem. Phys.* **1997**, *107*, 10029.
 (35) Alexandrova, A. N.; Boldyrev, A. I.; Fu, Y. J.; Yang, X.; Wang, X. B.; Wang, L. S. *J. Chem. Phys.* **2004**, *121*, 5709.
 (36) Alexandrova, A. N.; Boldyrev, A. I. *J. Chem. Theory Comput.* **2005**, *1*, 566.
 (37) Becke, A. D. *Phys. Rev. A* **1988**, *38*, 3098.
 (38) Lee, C. T.; Yang, W. T.; Parr, R. G. *Phys. Rev. B* **1988**, *37*, 785.
 (39) Frisch, M. J.; et al. *Gaussian 03*, revision C.02; Gaussian, Inc.: Wallington, CT, 2003.
 (40) Dunning, T. H., Jr.; Hay, P. T. In *Modern Theoretical Chemistry*; Schaefer, H. F., Ed.; New York, 1976; Vol. 3, p 1.
 (41) Weigend, F.; Ahlrichs, R. *Phys. Chem. Chem. Phys.* **2005**, *7*, 3297.
 (42) Pople, J. A.; Head-Gordon, M.; Raghavachari, K. *J. Chem. Phys.* **1987**, *87*, 5968.

- (43) Reed, A. E.; Weinstock, R. B.; Weinhold, F. *J. Chem. Phys.* **1985**, *83*, 735.
 (44) Bickelhaupt, F. M.; Baerends, E. J. In *Reviews in Computational Chemistry*; Lipkowitz, K. B., Boyd, D. B., Eds.; Wiley-VCH: New York, 2000; Vol. 15, p 1.
 (45) Morokuma, K. *Acc. Chem. Res.* **1977**, *10*, 294.
 (46) Ziegler, T.; Rauk, A. *Theor. Chim. Acta* **1977**, *46*, 1.
 (47) Baerends, E. J.; et al. *ADF2008.01*; Scientific Computing and Modelling NV, Theoretical Chemistry, Vrije Universiteit: Amsterdam, The Netherlands, 2008.
 (48) te Velde, G.; Bickelhaupt, F. M.; Baerends, E. J.; Fonseca Guerra, C.; van Gisbergen, S. J. A.; Snijders, J. G.; Ziegler, T. *J. Comput. Chem.* **2001**, *22*, 931.
 (49) Perdew, J. P. *Phys. Rev. B* **1986**, *33*, 8822.
 (50) Kutzelnigg, W.; Fleischer, U.; Schindler, M. The IGLO-Method: Ab-Initio Calculation and Interpretation of NMR Chemical Shifts and Magnetic Susceptibilities. In *NMR, Basic Principles and Progress*; Diehl, P.; Fluck, E.; Günther, H.; Kosfeld, R.; Seelig, J., Eds.; Springer-Verlag: Berlin, Heidelberg, 1990; Vol. 23, pp 165–262.
 (51) Kutzelnigg, W. *Isr. J. Chem.* **1980**, *19*, 193.
 (52) Koster, A. M.; Flores-Moreno, R.; Gaudner, G.; Goursot, A.; Heine, T.; Patchkovskii, S.; Reveles, J. U.; Vela, A. *deMon*; deMon Developers Community: Mexico, 2000.
 (53) Malkin, V. G.; Malkina, O. L.; Salahub, D. R. *Chem. Phys. Lett.* **1993**, *204*, 80.

Scheme 1



perpendicular to the Si_5 plane. VU was employed for the visualization of molecular fields.

Structures

Si_5H_5^- might be considered as the heavier C_5H_5^- analogue. Korkin et al. demonstrated that the most stable Si_5H_5^- structure is not planar.⁵⁴ Nevertheless, let us consider a D_{5h} Si_5H_5^- framework as our starting point to describe the title cluster structure. Five protons can be formally removed from Si_5H_5^- to obtain Si_5^{6-} (see Scheme 1). This generates five lone pairs, one on each terminal silicon and pointing outward, roughly in the direction where the hydrogen nuclei were located at the D_{5h} Si_5H_5^- structure. Let us consider lithiums as counterions. The singlet D_{5h} structure **1-A** is an obvious choice. It has seven imaginary frequencies at the B3LYP/def2-TZVPP^{37,38,41} level, however. Note that as a result of the ionic character of its bonding, lithium may prefer bridging positions and, therefore, the structure perhaps does not follow classical considerations.^{55–57}

One of the imaginary frequencies connects **1-A** to a planar star-like structure **1-B** (Scheme 1). The latter structure is approximately $60 \text{ kcal}\cdot\text{mol}^{-1}$ more stable than **1-A**, but it has still two imaginary frequencies. To identify the lowest-energy structure, we used the novel GEGA technique developed by Alexandrova and Boldyrev.^{35,36}

The isomers found within $10 \text{ kcal}\cdot\text{mol}^{-1}$ above the global minimum (at the CCSD(T)⁴²/def2-TZVPP//B3LYP/def2-TZVPP level) are shown in Figure 1. Our results reveal that the most stable Si_5Li_5^- isomer is a singlet C_{2v} structure (**1-C**) and is approximately $3.4 \text{ kcal}\cdot\text{mol}^{-1}$ lower in energy than the second most stable alternative (C_{2v} , **1-D**). Interestingly, both latter structures consist of two Li^+ cations coordinated above and below a planar Si_5^{6-} unit, respectively, with three bridging lithiums located in the silicon ring plane. Double-bridged structures, **1-E** and **1-F**, were also found, but they are less stable than **1-C** by 7.0 and $11.3 \text{ kcal}\cdot\text{mol}^{-1}$, respectively. The most stable triplet structure is $23.7 \text{ kcal}\cdot\text{mol}^{-1}$ higher in energy than **1-C**, which excludes further consideration of high-spin species (see Figure 4-SI).

Of course, numerous possible structures become available as the number of lithium atoms increases. The global minimum structures of Si_5Li_6 and Si_5Li_7^+ , located using GEGA, are shown

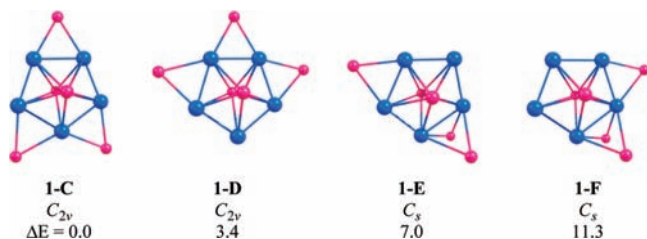
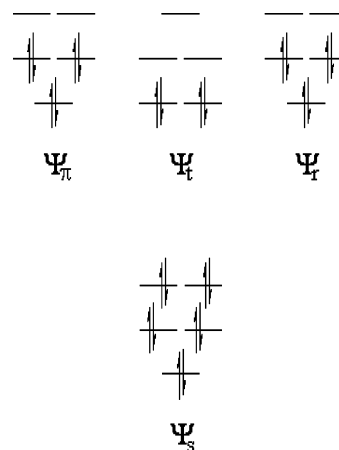


Figure 1. Isomers for Si_5Li_5^- . Relative energies calculated at the CCSD(T)/def2-TZVPP//B3LYP/def2-TZVPP level with respect to structure **1-C** in $\text{kcal}\cdot\text{mol}^{-1}$. The pink and blue balls represent lithium and silicon atoms, respectively.

Scheme 2



in Figure 2. (Higher-energy isomers found using GEGA are shown in Figures 1-SI, 2-SI, and 3-SI.) The C_{2v} structure (**2-A**) is the most stable form for Si_5Li_6 , while the D_{5h} structure (**3-A**) is the global minimum isomer for Si_5Li_7^+ . The next lowest-energy isomers of Si_5Li_6 and of Si_5Li_7^+ are 7.1 and $9.6 \text{ kcal}\cdot\text{mol}^{-1}$ higher in energy than **2-A** and **3-A**, respectively. In both global minimum structures, the lithium atoms occupy the empty bridge positions around the silicon ring in the Si_5Li_5^- framework. The resulting structures are beautiful six- and seven-peak molecular stars.

Let us highlight some general structural trends of the $\text{Si}_5\text{Li}_n^{n-6}$ systems ($n = 5, 6, 7$): (1) Opposite to Si_5H_5^- , the silicon ring in the lithium analogues is planar. (2) The Si–Si bond distances of 2.32 – 2.44 \AA are in the range of a conventional single Si–Si bond (2.35 \AA for Si_2H_6). (3) The shortest Si–Si distances are found between those silicon atoms that are not involved in a bridge. (4) The apical Si–Li distances are longer than the equatorial Si–Li ones. (5) Finally, the Li–Si distances of 2.37 – 2.64 \AA are shorter than the average Li–Si bond length (2.68 \AA) in the hexamer $(\text{Me}_3\text{SiLi})_6$.⁵⁸

Bonding

The charges on lithium are in the range of $+0.73|e|$ to $+0.92|e|$, respectively, according to the natural population analysis (NPA).⁴³ From the charge distribution it follows that the apical lithium atoms are more positive than the equatorial ones. These large positive natural charges on the lithium atoms stress the dominant Li–Si ionic interactions in the title complexes. Interestingly, the charge of the silicon ring increases

(54) Korkin, A.; Glukhovtsev, M.; Schleyer, P. v. R. *Int. J. Quantum Chem.* **1993**, *46*, 137.

(55) Gregory, K.; Schleyer, P. v. R.; Snaith, R. *Adv. Inorg. Chem.* **1991**, *37*, 47.

(56) Schleyer, P. v. R. *Pure Appl. Chem.* **1984**, *56*, 151.

(57) Setzer, W. N.; Schleyer, P. v. R. *Adv. Organomet. Chem.* **1985**, *24*, 353.

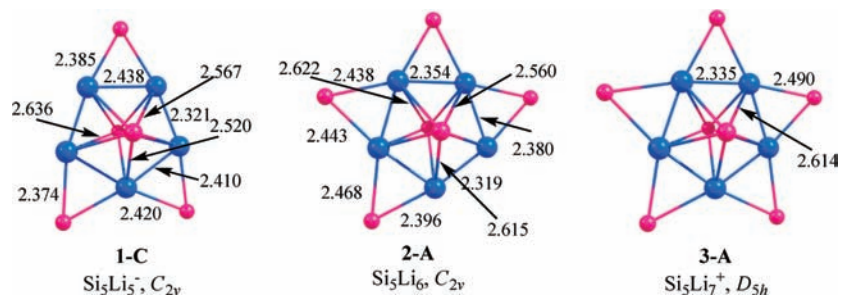


Figure 2. Lowest-energy structures of Si_5Li_5^- , Si_5Li_6 , and Si_5Li_7^+ calculated at the B3LYP/def2-TZVPP level. Bond lengths in Å.

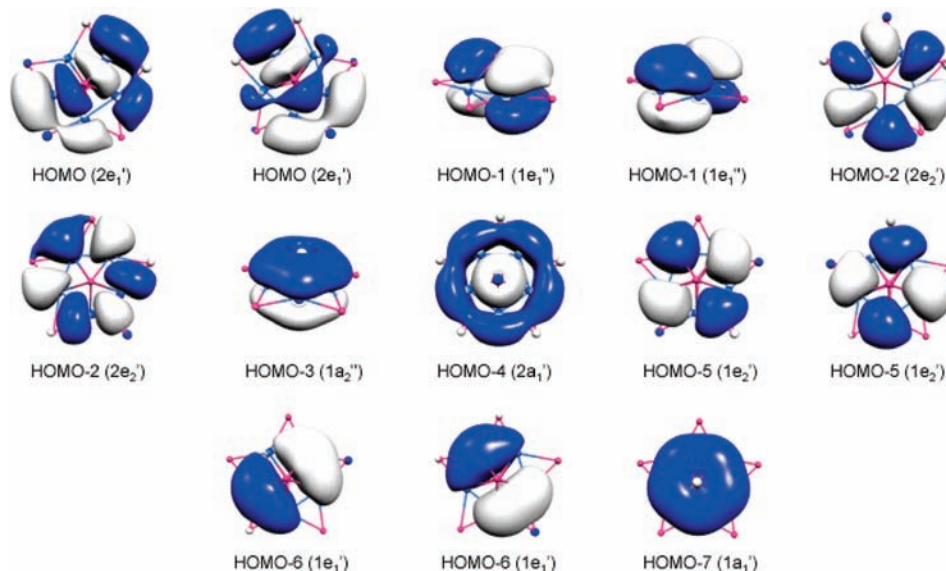


Figure 3. Molecular orbitals of Si_5Li_7^+ .

from Si_5Li_5^- (-5.01eV) to Si_5Li_7^+ (-5.40eV), indicating that the bonding in latter complexes is more ionic. Thus, the global minimum structures depicted in Figure 2 comprise, essentially, the Si_5^{6-} ring interacting with lithium cations.

As mentioned previously, the Si–Si bond distances in the star-like structures lie within the range of conventional single Si–Si bonds. However, Si–Si Wiberg bond indices (WBI), a measure of formal chemical bond orders, show the Si–Si bond order ranges from 1.32 to 1.39, which are higher than the corresponding value calculated for a typical single Si–Si bond in Si_2H_6 (WBI = 1.03). This pinpoints a significant electron delocalization within the silicon ring. In contrast, the low values of calculated Si–Li WBI (<0.2) support the presence of the dominant Li–Si ionic interactions. Interestingly, the total WBI of the silicon atoms vary between 3.28 and 3.33; thus, the octet rule is not violated, despite the hypercoordination.

To gain a quantitative insight into the nature of the Si–Li interactions in Si_5Li_7^+ , we additionally used EDA.^{45,46} The results obtained for the bridged (**3-A**) and nonbridged structures (**3-B**) were compared. Both isomers are local minima on the corresponding potential energy surfaces and possess a D_{5h} symmetry. **3-B** is less stable than **3-A** by $25.9\text{ kcal}\cdot\text{mol}^{-1}$. As any partitioning-energy scheme, the main issue is defining the proper fragments.⁴⁴ The molecule, of course, does not care; it will make whatever electron shifts it needs to maximize bonding. Let us consider the $\text{Si}_5\text{Li}_2^{4-}$ and Li_5^{5+} units as appropriate

fragments to analyze the in-plane equatorial $\text{Si}\cdots\text{Li}$ bonding interactions. EDA results are summarized in Table 1. As expected, the calculations predict that the interaction energy between $\text{Si}_5\text{Li}_2^{4-}$ and Li_5^{5+} is higher for **3-A** than for **3-B** by $92\text{ kcal}\cdot\text{mol}^{-1}$. Certainly, in both complexes the largest component of the attraction is the electrostatic term, ΔV_{elstat} , but this term is higher for the bridged structure by $44\text{ kcal}\cdot\text{mol}^{-1}$. Note that upon formation of the bridged structure, the Pauli repulsion term ΔE_{Pauli} decreases by $\sim 17\text{ kcal}\cdot\text{mol}^{-1}$. The orbital contribution ΔE_{oi} is clearly weaker than the electrostatic attraction, but going from **3-B** to **3-A**, the ΔE_{oi} value increases by $30.7\text{ kcal}\cdot\text{mol}^{-1}$. Thus, the ionic character of the Si–Li interactions induces the formation of a bridged structure,

Table 1. EDA of Si_5Li_7^+ at the BP86/TZ2P Level^a

	3-A	3-B
ΔE_{int}	−1430.3	−1338.2
ΔE_{Pauli}	104.9	122.2
ΔV_{elstat}	−1389.8	−1345.8
ΔE_{oi}	−145.3	−114.6

^a Energies are given in $\text{kcal}\cdot\text{mol}^{-1}$.

(58) Schaff, T. F.; Butler, W.; Glick, M. D.; Oliver, J. P. *J. Am. Chem. Soc.* **1974**, *96*, 7593.

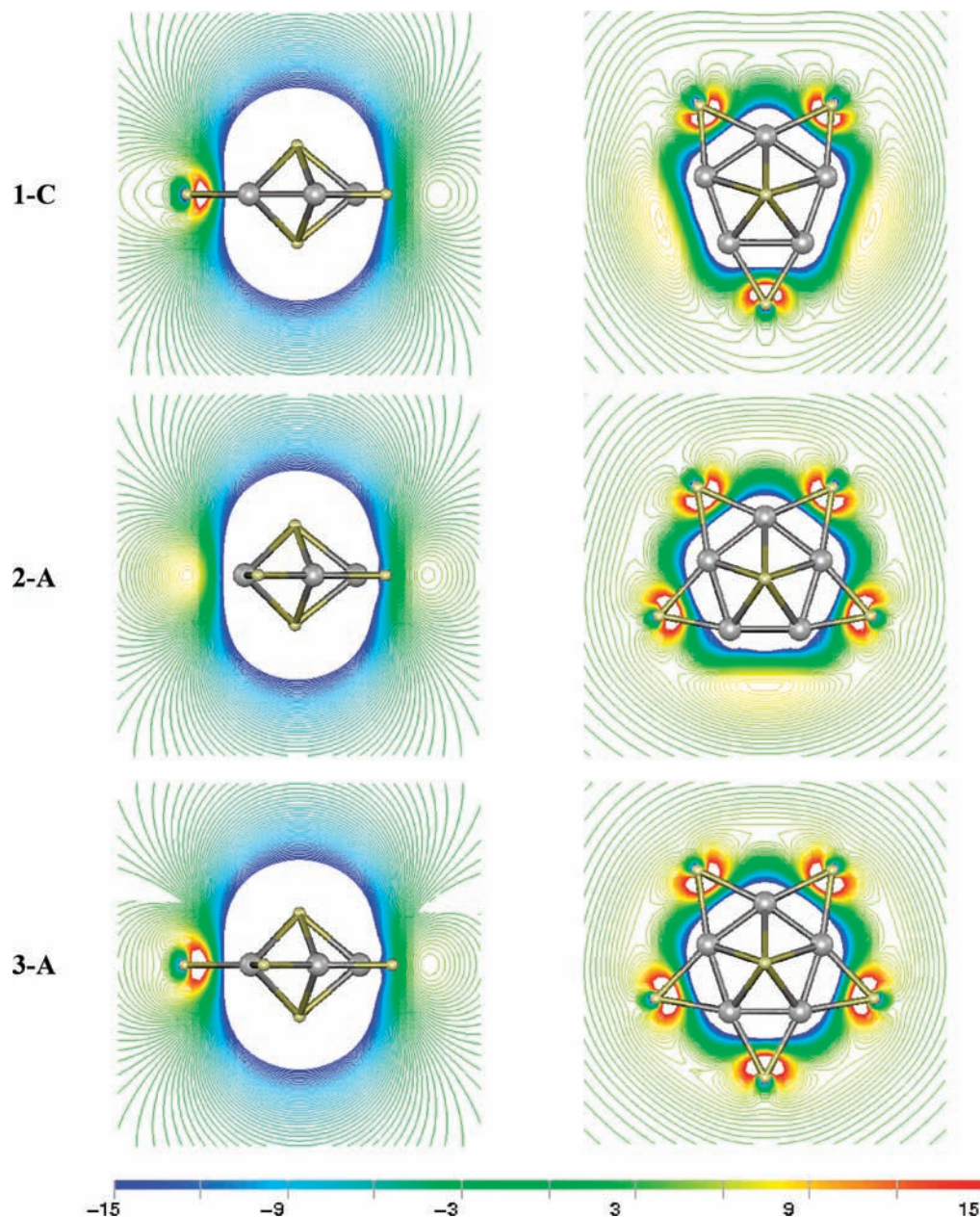


Figure 4. z -component of \mathbf{B}^{ind} , shielding (diatropic, blue) or enforcing (paratropic, red) the external field, shown in the molecular plane and perpendicular to it.

but concomitantly our calculations show that the reduction of the Pauli repulsion and the maximization of the orbital contribution are also significant for the star-like structure formation.

Let us look at the molecular orbitals. For the sake of brevity, we only consider Si_5Li_7^+ . The highest occupied molecular orbital (HOMO) of Si_5Li_7^+ is a doubly occupied degenerate σ orbital set ($2e_1'$). There are six π -electrons in all the star-like structures discussed here. They are distributed in the HOMO-1 (a $1e_1''$ degenerate π orbital set) and the HOMO-3 ($1a_2''$). As in cyclopentadienyl or benzene, the $\text{Si}_5\text{Li}_n^{n-6}$ system planarity can be ascribed to the stabilization of highly delocalized six π electrons and six σ -type radial electrons (see Figure 3). However, it is interesting to point out that this differs from Si_5H_5^- where there are also six π electrons, but the D_{5h} structure is not a local minimum.

Consequently, what is the role of lithium in the Si_5 ring planarization? To explore further this point, we have taken the

Si_5Li_7^+ structure and replaced all seven lithium atoms by point charges $q = 1$, located at the positions of each of the lithium nuclei. Then, the structure of the central Si_5^{6-} unit has been optimized. Si_5^{6-} is a local minimum at the B3LYP/def2-TZVPP level. The optimized structure retains the planarity found for the Si_5 unit of Si_5Li_7^+ , with a Si-Si bond length of 2.513 Å, which is slightly longer than the Si-Si bond lengths at the $\text{Si}_5\text{Li}_n^{n-6}$ systems ($n = 5, 6, 7$).

Now, the inspection of the MOs of Si_5^{6-} reveals that its 26 valence electrons are arranged as depicted in Scheme 2. Namely, the central Si_5^{6-} structural unit comprises a 2-fold aromatic system, one 6-electrons π -aromatic system, and one 6-electrons σ -aromatic system. Additionally, the tangential molecular orbitals conform a 4-electron nonaromatic system. Consequently, the MO analysis of the model system suggests that the role of the lithium atoms is to provide the precise number of electrons to the central Si_5 unit, i.e., to fill both the π and radial aromatic

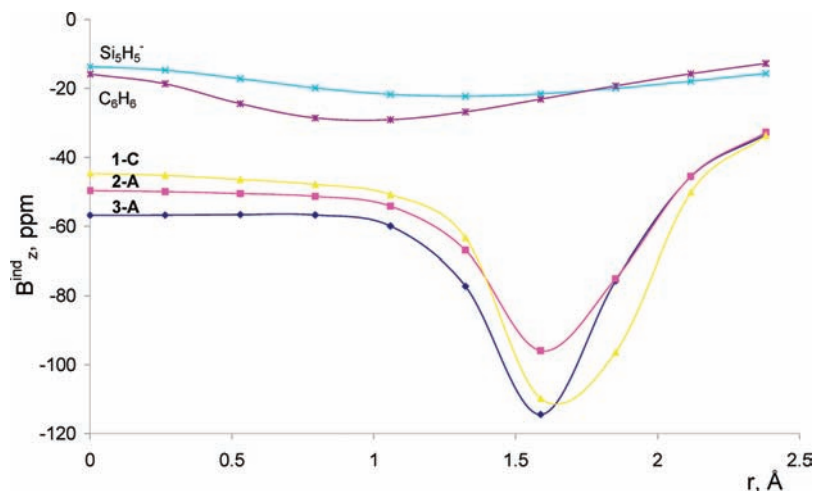


Figure 5. B_z^{ind} profiles of Si_5Li_5^- , Si_5Li_6 , Si_5Li_7^+ , Si_5H_5^- , and C_6H_6 calculated at the PW91/IGLO level.

systems with six electrons. The advantages of the planarity of the Si_5 ring stem, therefore, form the 2-fold aromatic stabilization of its electronic structure. Naturally, strong donor substituents, such as lithium, are required to bring about such aromatic stabilization.

Aromaticity

The aromatic stabilization hypothesis pointed out in the previous section will be assessed further by an in-depth analysis of the induced magnetic field \mathbf{B}^{ind} .^{59,60} Figure 4 depicts the contour lines of the z -component of the induced magnetic field, B_z^{ind} , for **1-C**, **2-A**, and **3-A** (Please refer to the Computational Details). Note that B_z^{ind} for an external field perpendicular to the ring is equivalent to the NICS_{zz} .^{61–63} The shielding cones of the silicon clusters above and below the ring are comparable in shape to those of benzene,⁶⁰ even though they are larger in magnitude and extension. Around the σ -framework of Si_5^{6-} , there are five paratropic regions (one at each of the sides of the pentagon). This behavior does not depend on the number of cations and is a clear consequence of the strong electron delocalization as in benzene.⁶⁰

The B_z^{ind} value at the center of the Si_5 ring (let us call it as $B_z^{\text{ind}}(0)$ in analogy to $\text{NICS}(0)$) in Si_5Li_7^+ is higher than -44 ppm, which absolute value is approximately 3 times larger than that in benzene (-15.9 ppm). The corresponding value for the D_{5h} Si_5H_5^- structure is only -13.7 ppm; thus, it is apparent that substitution of hydrogen for lithium intensifies electron delocalization into the Si ring. Note that $B_z^{\text{ind}}(0)$ increases from Si_5Li_7^+ (-56.8 ppm) to Si_5Li_5^- (-44.7 ppm). Interestingly, the B_z^{ind} profiles of **1-C**, **2-A**, and **3-A** show a minimum at the position of the apical lithium atoms. In summary, the magnetic properties show that the significant electron delocalization enhances the stability of the structures proposed here and render them amenable to experimental detection.

Acknowledgment. The work in Guanajuato is supported by the Air Force Research Laboratory *Latin American Initiative Project*, and Conacyt (Grant 57892). We thank Roberto Flores-Moreno, Keigo Ito, and Maryel Contreras for cheerful discussions. W.T. thanks Fondecyt for its postdoctoral fellowship (Grant 3080042). N.P. and R.I. acknowledge Conacyt for the Ph.D. fellowship. A.T.-L. acknowledges FONDECYT (Grant 1090460) and FONDAP (Grant 11980002 CIMAT) for financial support.

Supporting Information Available: Full citation of refs 39 and 47 and Cartesian coordinates of all title species. This material is available free of charge via the Internet at <http://pubs.acs.org>.

JA903694D

- (59) Heine, T.; Islas, R.; Merino, G. *J. Comput. Chem.* **2007**, *28*, 302.
 (60) Merino, G.; Heine, T.; Seifert, G. *Chem.—Eur. J.* **2004**, *10*, 4367.
 (61) Corminboeuf, C.; Heine, T.; Seifert, G.; Schleyer, P. v. R.; Weber, J. *Phys. Chem. Chem. Phys.* **2004**, *6*, 273.
 (62) Chen, Z. F.; Wannere, C. S.; Corminboeuf, C.; Puchta, R.; Schleyer, P. v. R. *Chem. Rev.* **2005**, *105*, 3842.
 (63) Fallah-Bagher-Shaidaei, H.; Wannere, C. S.; Corminboeuf, C.; Puchta, R.; Schleyer, P. v. R. *Org. Lett.* **2006**, *8*, 863.